The hydrophobic film displayed here as a space-filling model protects iron surfaces (ball-and-stick model) from corrosion. The protective coat is formed by an elegant multifunctional organic additive, and demonstrates how even simple molecules can perform technologically important tasks.

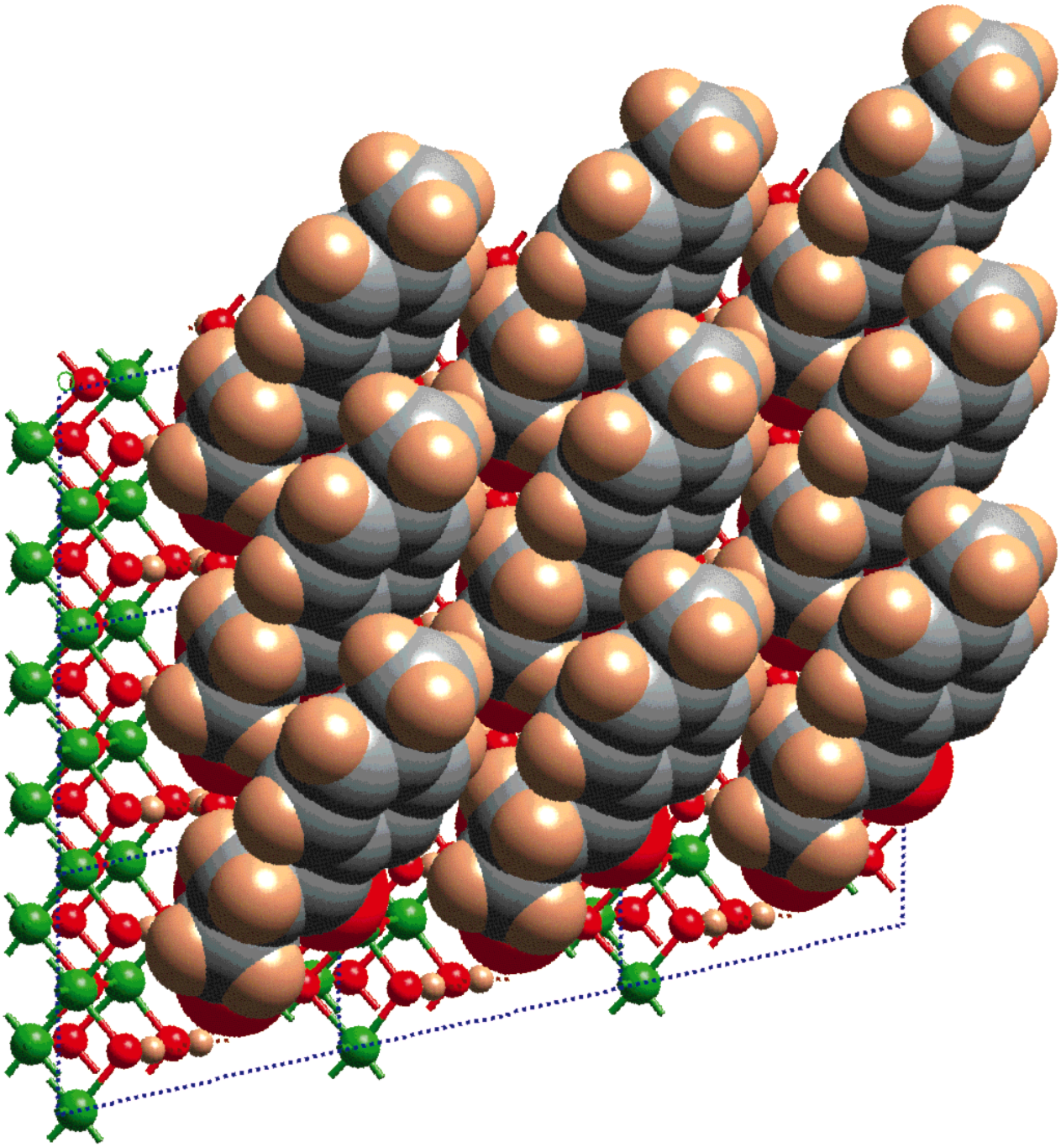

Find out more on the following pages.

  1433-7851/98/3723-3245 $ 17.50+.50/0

Modeling Surface Engineering: Use of Polymetallic Iron Cages and Computer Graphics To Understand the Mode of Action of a Corrosion Inhibitor**

Marcus Frey, Steven G. Harris, Jeremy M. Holmes, David A. Nation, Simon Parsons, Peter A. Tasker,* Simon J. Teat, and Richard E. P. Winpenny*

The protection of metals from atmospheric corrosion is a major factor determining their usefulness, for example as construction materials.[1] As a consequence, most coatings for metals contain corrosion inhibitors as key constituents.[2] Chromates and other inorganic materials have proved effective in such a role, but their toxicity now restricts their use and more benign organic alternatives are being sought.[3] It can be envisaged that functionalized forms of such organic active species will allow surface engineering and could, for example, cross-link into polymer coatings to give improved adhesion. Despite the importance of organic surface modifiers, little attention has been paid to how they bind to oxidized metal surfaces, and why seemingly minor modifications in the structures of organic active compounds can have a profound effect on their efficacy. Here we illustrate a new approach, based on the synthesis of polymetallic complexes involving known organic active compounds, and the use of structural motifs found in such complexes to model relevant surface-active interactions, and hence understand the modes of action of known corrosion inhibitors.

The specific project chosen to demonstrate this approach involves a powerful corrosion inhibitor produced by Ciba Specialty Chemicals. The active ingredient, which is used in water-borne coatings for mild steel, is 3-(4-methylbenzoyl)-propionic acid (HL). It is thought to bind to oxidized iron surfaces in the deprotonated form to create a passivating film. Extensive testing of this compound and related derivatives as corrosion inhibitors in protective coatings[4] indicates that both the presence of the methyl group in the *para* position of the aromatic ring and the carbonyl group greatly increase the usefulness of the active compounds over organic molecules without the ketone functionality and with different types and positions of aromatic substituents.

Model iron complexes of L^- were made by procedures derived from work by Lippard and co-workers.[5, 6] Two structures are relevant.[7] Firstly, a decanuclear "ferric wheel" of formula $[\{Fe(OMe)_2(L)\}_{10}]$ (**1**), in which iron(III) centers are bridged by methoxide and L^- groups (Figure 1). Previous decanuclear iron(III) wheels have been reported with chloroacetate[5] and acetate ligands.[8] The second structure, the undecanuclear cage $[Fe_{11}(O)_6(OH)_6(L)_{15}]$ (**2**, Figure 2), is more complex and involves six iron centers (Fe3, Fe4, Fe6, Fe7, Fe9, Fe10) which describe a trigonal prism. This prism is then capped by two further iron atoms (Fe1, Fe2) on the triangular faces and three iron atoms (Fe5, Fe8, Fe11) on the rectangular faces. There are six μ_3-oxide oxygen atoms, which lie within the metal polyhedron, and six μ_3-hydroxide groups, which lie on the surface of the polyhedron. Carboxylate ligands complete the coordination spheres of each iron. A similar cage has been reported with benzoate.[6] Fe–O bond lengths in **1** are unremarkable; in **2** the Fe–O(oxide) bond distances are markedly shorter than Fe–O(hydroxide) dis-

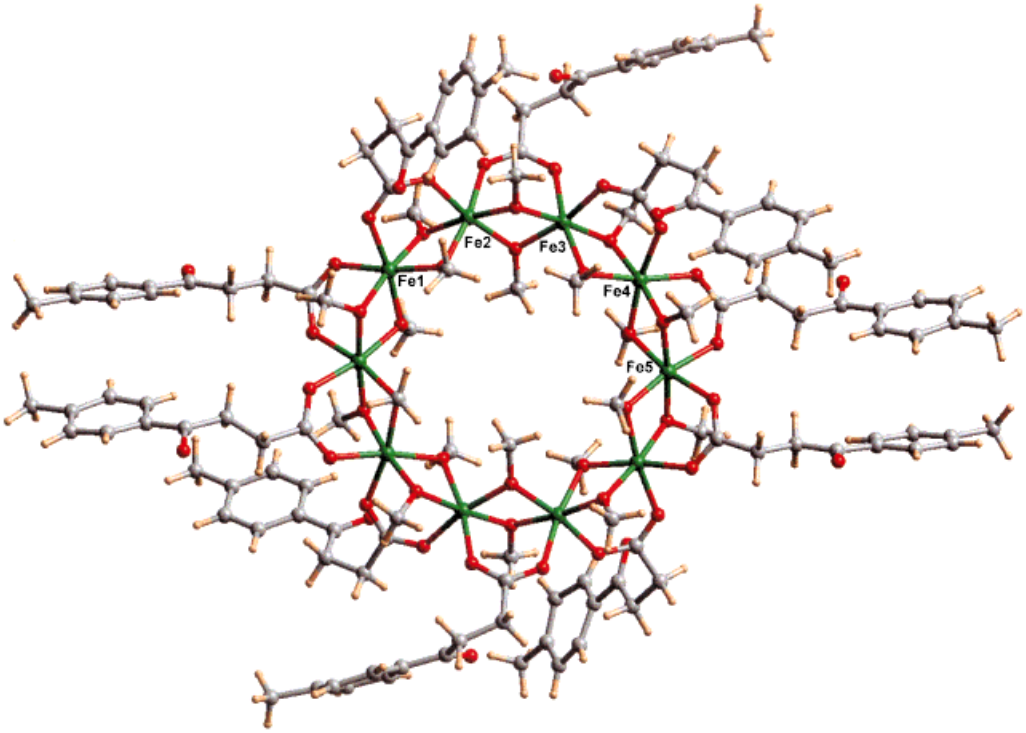

Figure 1. The structure of $[\{Fe(OMe)_2L\}_{10}]$ in the crystal, showing the bonding of the carboxylate head group to the Fe centers and that the ketone functionality of L is not involved (Fe: green, O: red, C: grey, H: light brown; these colors are also used in Figures 2–4). Bond lengths [Å]: Fe–O(methoxide) 1.962–2.000, Fe–O(L) 2.004–2.064 (esd 0.012); bond angles [°]: *cis* angle at Fe 77.3–99.9, *trans* angle at Fe 168.0–175.5 (esd 0.5).

[*] Prof. P. A. Tasker, Dr. R. E. P. Winpenny, S. G. Harris, Dr. J. M. Holmes, Dr. D. A. Nation, Dr. S. Parsons
Edinburgh Centre for Surface Coordination Chemistry
Department of Chemistry, The University of Edinburgh
West Mains Road, Edinburgh, EH9 3JJ (UK)
Fax: (+44) 131-650-4743

Dr. M. Frey
Ciba Specialties, Basel (Switzerland)

Dr. S. J. Teat
CCLRC Daresbury Laboratory,
Daresbury, Warrington, Cheshire, WA4 4AD (UK)

[**] This work was supported by Ciba Specialty Chemicals, the EPSRC (UK), the Royal Society of London, and Zeneca Specialties. We thank Prof. W. Clegg for help with the synchrotron X-radiation study.

  1433-7851/98/3723-3246 $ 17.50+.50/0

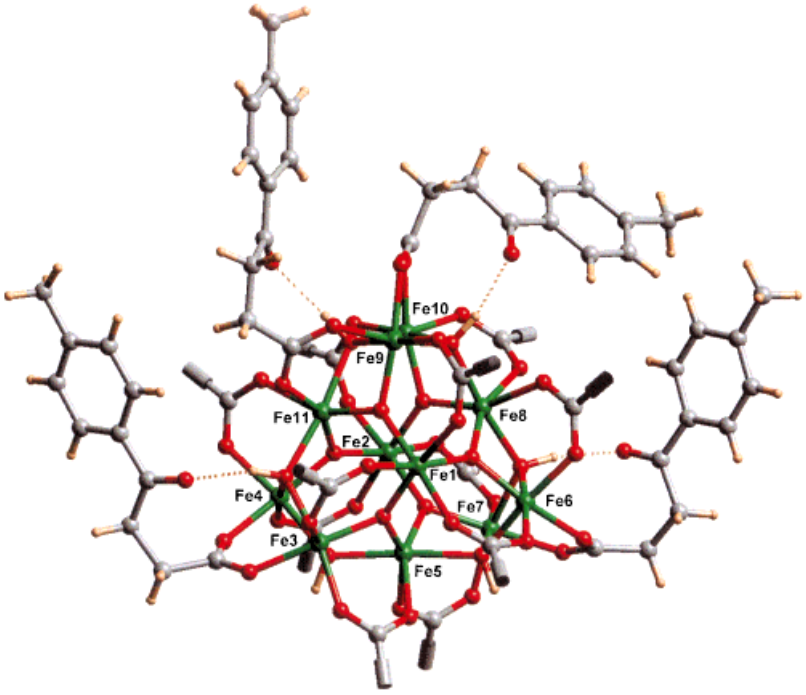

Figure 2. The structure of $[Fe_{11}(O)_6(OH)_6(L)_{15}]$ in the crystal, viewed along the trigonal axis of the metal polyhedron. The organic tail group of eleven of the L^- ligands is excluded for clarity. The four L ligands shown have hydrogen bonds, shown as dotted lines, to hydroxide groups bridging the metal core. Bond lengths [Å]: Fe–O(oxide) 1.878–1.941, Fe–O(hydroxide) 2.049–2.176, Fe–O(L) 1.936–2.158 (esd 0.008); bond angles [°]: *cis* angle at Fe 75.9–109.3, *trans* angle at Fe 154.6–177.4 (esd 0.3).

tances, which allows clear differentiation between these two ligand types. In both structures all Fe sites have approximately octahedral coordination geometries.

In both compounds L^- binds to the iron atoms exclusively through the carboxylate functionality, which spans metal–metal vectors in a 1,3-bridging mode. The ketone functionality does not bind to metal sites, and in **1** plays little part in the structure. In **2** the ligand again binds to the iron centers through the carboxylate group, but now the ketone plays a much more significant role. Four of the fifteen L^- ligands have hydrogen bonds between the ketone oxygen atom and a bridging hydroxide group of the cage (Figure 2). The structures of the model complexes suggest that the presence of the ketone in L^- enhances the performance of the corrosion inhibitor due to this ability to bind to hydroxide groups on a metal oxide hydroxide surface, while the carboxylate binds to the metals. This simple organic molecule is showing bifunctional recognition of the metal surface. To demonstrate that this ditopic binding mode is not a function of crystallization, **2** was also crystallized from EtOH and the structure analyzed.[7] Unfortunately the small crystals which resulted diffracted weakly and synchrotron radiation was required to obtain any data, which even then were of marginal quality. The metal cage in these crystals is identical to **2** when crystallized from MeCN; however, the paucity of observed data and severe disorder in the lattice solvent has prevented refinement of this structure reaching convergence, and we only report unit cell constants here together with the important conclusion that the cage structure is independent of crystallization solvent.

This proposed mode of action receives further support from computer modeling. Bravais–Friedel–Donnay–Harker theory[9] suggests that for lepidocrocite, which is the most common iron oxide hydroxide found on surfaces,[10] the {020}, {021}, and {110} Miller planes are responsible for 94% of the total surface area. Predicting the structures of corroded surfaces is difficult, and the assumptions involved in choosing this mineral seem as valid as any; similar results to those described below can be obtained for the (001) plane of magnetite or the (110) plane of goethite. These three phases—lepidocrocite, magnetite, and goethite—are those detected in rust samples.[10] Layers coplanar with the (021) plane contain iron(III) and hydroxide sites with very similar dispositions to those found in **2**. One molecule of L^- was attached to this (021) surface, using the bonding mode found in **2**, and the energy-minimized conformation for the organic molecule calculated (Figure 3).[11] This leads to the tolyl group of L^- lying at an angle of 48° to the metal oxide surface. When this orientation was used in a computer-generated monolayer, very good surface coverage is obtained (Figure 4) with efficient packing (ca. 50 $Å^2$ per L^-). Few gaps are found between L^- units, giving a

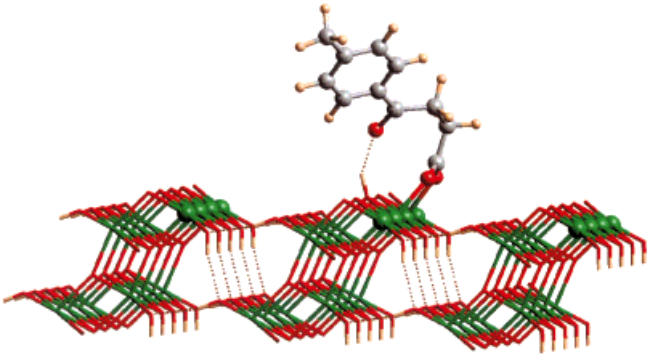

Figure 3. The bonding mode of a single molecule of L^-, derived from **2**, used to address the surface of lepidocrocite.

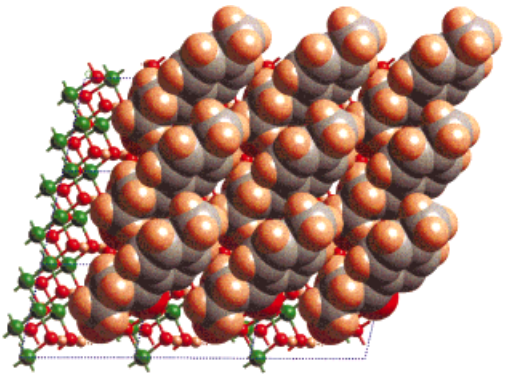

Figure 4. The packing of nine L^- ligands on the (021) surface of lepidocrocite based on the bonding mode found in the structure of $[Fe_{11}(O)_6(OH)_6(L)_{15}]$. For each L^- unit the carboxylate group is at the bottom left of the molecule as viewed, and the methyl group is at the top right.

  1433-7851/98/3723-3247 $ 17.50+.50/0

surface which is hydrophobic and provides a barrier to ingress and egress of ionic species aiding corrosion. If the *para*-methyl group is absent from the tolyl ring the integrity of the barrier is diminished. Also, if the aromatic ring is substituted in different positions (e.g. *ortho* or *meta*) it is much more difficult to retain the bifunctional mode of attachment and close packing of ligands on the surface due to repulsion between the aromatic substituents of neighboring molecules.

Ligand L^- is therefore an extremely elegant multifunctional additive with three aspects to its utility: firstly, binding of the metal sites by the carboxylate head group; secondly, hydrogen bonding between the ketone and the hydroxide group on the metal oxide hydroxide surface; thirdly, the extremely efficient packing of the organic molecules above this surface, forming a well-integrated protective coat. While the first function is predictable based on known coordination chemistry of carboxylates, the other two functions could only be demonstrated by the combination of characterization of model complexes and computer modeling of the additive-surface interaction. The information gained from such studies will enable the design of further actives for modification of metal surfaces with a wide range of industrial applications.

Experimental Section

1: Hydrated ferric nitrate (0.93 g, 2.3 mmol) was allowed to react with Na(L) (0.49 g, 2.3 mmol) in MeOH (20 mL) to give a yellow powder in 85% yield, which was crystallized from DMF/MeOH to give a small quantity of yellow crystals. Elemental analysis calcd for $C_{130}H_{170}Fe_{10}O_{30}$: C 50.51, H 5.54; found: C 50.30, H 5.53.

2: Hydrated ferric nitrate (3.23 g, 8.0 mmol) was allowed to react with Na(L) (4.01 g, 18.7 mmol) in H_2O (100 mL) to give a light orange powder in 90% yield, which was analyzed to be the trinuclear species $[Fe_3(O)(L)_6(H_2O)_3]\cdot L$. Elemental analysis calcd for $C_{77}H_{83}Fe_3O_{25}$: C 58.68, H 5.31; found: C 59.69, H 5.23. The powder was redissolved in MeCN (20 mL), and, on allowing diethyl ether to diffuse into the solution, orange-brown crystals formed in the solution after several days. The compound could also be crystallized by being redissolved in EtOH (20 mL) followed by diffusion of diethyl ether into the solution.

Received: July 20, 1998 [Z12181IE]
German version: *Angew. Chem.* **1998**, *110*, 3435 – 3439

Keywords: clusters · corrosion · iron · surface chemistry

[1] T. W. Swaddle, *Inorganic Chemistry: An Industrial and Environmental Perspective*, Academic Press, London, **1997**.
[2] K. Doren, W. Freitag, D. Stoye, *Water-Borne Coatings: The Environmentally Friendly Alternative*, Hanser/Gardner, Cincinnati, **1994**.
[3] Yu. I. Kuznetsov, *Organic Inhibitors of Corrosion of Metals*, Plenum, New York, **1996**.
[4] Ciba Specialty Chemicals, unpublished results.
[5] K. L. Taft, C. D. Delfs, G. C. Papaefthymiou, S. Foner, D. Gatteschi, S. J. Lippard, *J. Am. Chem. Soc.* **1994**, *114*, 823.
[6] S. M. Gorun, G. C. Papaefthymiou, R. B. Frankel, S. J. Lippard, *J. Am. Chem. Soc.* **1987**, *109*, 3337.
[7] Crystal data for $\mathbf{1}\cdot$MeOH: $C_{131}H_{174}Fe_{10}O_{51}$, $M_r = 3123$, triclinic, $P\bar{1}$, $a = 10.537(4)$, $b = 18.856(6)$, $c = 19.392(7)$ Å, $\alpha = 101.23(2)$, $\beta = 105.36(2)$, $\gamma = 94.96(2)^\circ$, $V = 3605(2)$ Å^3, $Z = 1$ (the molecule lies on an inversion center), $T = 150.0(2)$ K, crystal size $0.49 \times 0.16 \times 0.16$ mm, $\mu(Mo_{K\alpha}) = 1.06$ mm^{-1}. Crystal data for **2**: $C_4H_6O\cdot 3C_2H_3N\cdot 0.5H_2O$: $C_{175}H_{191}Fe_{11}N_3O_{58.5}$, triclinic, $P\bar{1}$, orange-brown lath, $a = 19.534(8)$, $b = 21.320(11)$, $c = 22.821(14)$ Å, $\alpha = 83.71(4)$, $\beta = 74.13(4)$, $\gamma = 80.67(3)^\circ$, $V = 9000(8)$ Å^3, $Z = 2$, $T = 220.0(2)$ K, crystal size $0.39 \times 0.27 \times 0.12$ mm, $\mu(Mo_{K\alpha}) = 0.94$ mm^{-1}. Compound **2** was also crystallized from EtOH: crystal data for $\mathbf{2}\cdot 4.22\,EtOH\cdot 1.22\,Et_2O\cdot 3.0\,H_2O$; $C_{178.32}H_{214.52}Fe_{11}O_{65.44}$, $M_r = 4019$, triclinic, $P\bar{1}$, $a = 20.786(3)$, $b = 22.024(3)$, $c = 22.247(3)$ Å, $\alpha = 74.133(3)$, $\beta = 79.199(3)$, $\gamma = 80.096(3)^\circ$, $V = 9544(2)$ Å^3, $Z = 2$, $T = 160.0(2)$ K, crystal size $0.48 \times 0.10 \times 0.08$ mm, $\mu(Mo_{K\alpha}) = 0.89$ mm^{-1}. Data for **1** and $\mathbf{2}\cdot C_4H_6O\cdot 3C_2H_3N\cdot 0.5H_2O$ were collected with a Stoe Stadi-4 diffractometer equipped with an Oxford Cryosystems low-temperature device. Data for $\mathbf{2}\cdot 4.22\,EtOH\cdot 1.22\,Et_2O\cdot 3.0\,H_2O$ were collected with a Bruker AXS SMART three-circle diffractometer equipped with a CCD detector installed on Station 9.8 at the CCLRC Daresbury synchrotron radiation source. Absorption corrections were applied with ψ-scan data for **1** (min./max. transmission for **1**: 0.455/0.585). All structures were solved by direct methods (SIR92, A. Altomare, G. Cascarano, C. Giacovazzo and A. Guagliardi, *J. Appl. Cryst.* **1993**, *26*, 343) and completed by iterative cycles of ΔF syntheses and full-matrix, least-squares refinement against F^2 (SHELXTL, Brucker AXS). Hydrogen atoms were included in the first two structures in calculated positions, riding on parent carbon atoms, with $U(H) = 1.2\,U_{eq}(C)$ for aromatic hydrogen atoms and $U(H) = 1.5\,U_{eq}(C)$ for methyl hydrogen atoms. In the first two structures disordered and part-weight solvate molecules were found in the lattice, which were modeled as MeOH in **1**, and Et_2O, MeCN, and H_2O in **2**. All non-hydrogen atoms within the cages were refined with anisotropic displacement parameters: for **1**: 564 parameters, $wR2 = 0.3773$ for 9265 unique data ($2\theta \le 45^\circ$), $R1 = 0.1257$ for 3919 observed reflections with $F_o > 4\sigma(F)$, max./min. residual electron density 0.596/ – 0.589 e Å^3; for **2**: 2160 parameters, $wR2 = 0.2501$ for 19121 unique data ($2\theta \le 42^\circ$), $R1 = 0.0872$ for 10180 observed reflections with $F_o > 4\sigma(F)$, max./min. residual electron density 0.907/ – 0.627 e Å^3. Crystallographic data (excluding structure factors) for the structures reported in this paper have been deposited with the Cambridge Crystallographic Data Center as supplementary publication no. CCDC-102414, -102415, and -102416. Copies of the data can be obtained free of charge on application to CCDC, 12 Union Road, Cambridge CB2 1EZ, UK (fax: (+44) 1223-336-033; e-mail: deposit@ccdc.cam.ac.uk).
[8] C. Benelli, S. Parsons, G. A. Solan, R. E. P. Winpenny, *Angew. Chem.* **1996**, *108*, 1967; *Angew. Chem. Int. Ed. Engl.* **1996**, *35*, 1825.
[9] R. Docherty, K. J. Roberts, E. Dowty, *Comput. Phys. Commun.* **1988**, *51*, 423, and references therein.
[10] S. Music, D. Dragcevic, S. Popovic, I. Czako-Nagy, *Croat. Chem. Acta* **1995**, *68*, 315.
[11] All calculations were performed on a Silicon Graphics Indigo2 workstation equipped with the BIOSYM/MSI molecular modeling package Cerius2. Bravais – Friedel – Donnay – Harker calculations predicted that for a single crystal of lepidocrocite the surface would comprise four Miller planes: {010} (occupying 42.61% of total surface area), {021} (29.04%), {110} (22.83%), {111} (5.52%). No suitable carboxylate binding sites were found on the (010) plane, therefore calculations proceeded with the (021) plane. Simulated cleavage of a crystal parallel to the (021) plane results in a surface model with alternating parallel rows of μ_3-hydroxide anions and five-coordinate square-pyramidal metal sites. Ligand L^- was then attached to neighboring ferric sites, with the result that the carbonyl group came into hydrogen-bonding proximity of a nearby μ_3-hydroxide group. The energy-minimized conformation for L^- was calculated with a fixed O–H ··· O(ketone) distance of 2.9 Å. This conformation was then used to generate a surface layer of L^-, as shown in Figure 4. Ligand L^- occupies an area of 50 Å^2 for monolayer coverage.

  1433-7851/98/3723-3248 $ 17.50+.50/0